

# Experimental Study on the Performance of Wet Thermoacoustic Engine with Modified Parallel Plate Stack Design

Md. Imrul Kayes, Md. Ashiqur Rahman

Bangladesh University of Engineering and Technology  
Department of Mechanical Engineering, Dhaka-1000, Bangladesh  
kayesimrul@me.buet.ac.bd; ashiquurrahman@me.buet.ac.bd

**Abstract** - The requirement of high onset temperature difference is a critical limitation of thermoacoustic engine, a potential green technology for power generation from low-grade heat. Wet thermo-acoustic engines (WTE) can solve this problem by utilizing phase change heat transfer and hence resulting in devices with low onset temperature difference and increased acoustic power density. However, the strategy for imbibing condensable liquid into the WTE is not yet adequately established. Therefore, a novel type of stack for the WTE is presented in this work which uses mesh screen packing both as a spacer between the parallel plates and as the liquid retaining component of the device. A systematic study of the performance of a quarter standing wave WTE is carried out by altering the mesh packing longitudinally (plate spacing) and peripherally (mesh packing density) for different mesh numbers using water and air at atmospheric condition. Optimization of the proposed stack configuration is examined in terms of the onset temperature difference and the generated acoustic power. Within the parametric space of the present study, the optimized design of the modified parallel stack is obtained at a low onset temperature difference of 13°C and acoustic power of 29 mW.

**Keywords:** Wet thermoacoustic engine, modified parallel plate stack, mesh screen, acoustic power, onset temperature difference.

## 1. Introduction

Thermo-acoustic engines produce mechanical power in the form of acoustic waves from heat energy utilizing thermo-acoustic effects [1]. They have no moving parts and generate no exotic gases, making them a potential green, maintenance-free approach for utilizing low-grade heat (e.g. waste heat [2], solar power [3], and so on). However, because of the intrinsic irreversibility necessary for engine operation, these engines normally operate at high temperatures ( $> 200^{\circ}\text{C}$ ). Raspet [4] observed that adding condensable vapor into the thermoacoustic engines can reduce the operating temperature below  $100^{\circ}\text{C}$  and Noda and Ueda [5] confirmed it experimentally using vaporized water and ethanol. These engines are referred to as wet thermoacoustic engines (WTE). Tsuda and Ueda [6] demonstrated that the temperature of acoustic onset is abruptly reduced at a certain humidity ratio, remaining constant for any higher humidity value. Meir [7] reported production of eight times more acoustic power by WTE while operating at a temperature difference 150–200 K lower than its dry equivalent. Nevertheless, there is no defined mechanism for imbibing condensable fluid into the WTE.

Furthermore, the shape of the stack, which is a core part of thermo-acoustic engines, has a significant impact on their performance. Yu [8] theoretically studied the effect of stack geometry of several regular stack shapes (pin-array, parallel stack, circular pores) and found an optimum ratio of hydraulic channel diameter to thermal penetration depth that results in the minimum onset temperature. Parallel plate stack exhibits excellent performance (next to pin-array) [8] and is easy to manufacture. Hariharan [9] investigated the effects of parallel stack geometry and resonator length on the performance of thermoacoustic engine. Ke [10] reported that the optimal plate spacing of parallel plate stacks is around 2~4 times the thermal penetration depth [1]. The effect of stack geometry on the performance of WTE is not explored yet.

Therefore, this study presents a novel, modified form of parallel plate stack with mesh screen as the packing material in the space between the plates. This addition of mesh screen packing can imbibe condensable liquid in WTE, which is commonly utilized in phase change heat pipes [11]. Because of the wicking ability and the enhancement of heat transfer surface, it can also improve the WTE cycle. A new parameter called mesh packing density is defined which is the percentage of the volume of the mesh screen to the overall volume at the space between two plates of the stack. Mesh packing density indicates the variation of mesh screen packing in this modified parallel plate stack. The effects of the

variation of the geometrical parameters of the modified parallel stack such as plate spacing, mesh number, and mesh packing density are investigated with constant heating power and at atmospheric operating condition using air and water in a quarter standing wave WTE. Finally, the performance of the various configurations of the modified stack is evaluated in terms of the onset temperature difference and acoustic power to obtain the optimized design parameters.

## 2. Wet Thermoacoustic Cycle

A WTE produces its acoustic power when gas interacts with wet solid wall of narrow channel close to wavelength possessing a temperature gradient. Gas molecules gain heat and mass (vapor) from the hot end of the stack and reject them at the cold end, creating thermal expansion and contraction, respectively. This expansion and rejection induce a density difference along the stack and generate movement of the gas and vapor mixture. This cycle, as depicted in Fig. 1(a), is repeated at a quicker pace across the stack, resulting in acoustic power. The wet solid wall which acts as a storage for heat and liquid is called the stack and it is the heart of the WTE. Based on the governing equations derived by Raspert [7], Senga [12] divided the work sources of WTE into dissipative and energy conversion components. Viscosity, heat diffusion, and mass diffusion all cause dissipation, which are referred to as viscous resistance, thermal relaxation loss, and mass relaxation loss, respectively. Energy conversion for gas, as well as evaporation and condensation, are included in the energy components. Self-oscillation initiates in the engine when energy components surpass dissipative components. This occurs when a particular temperature difference, known as the onset temperature difference, is achieved. The molar ratio of condensable vapor and gas influences both the mass relaxation loss and energy components of evaporation and condensation.

## 3. Modified Parallel Plate Stack

Parallel-plate stacks are made of an array of parallel plates arranged in the direction of acoustic wave generation. The hydraulic radius, or  $r_h$ , is defined as the area parallel to the direction of the acoustic wave in a narrow channel divided by the wetted parameter and is used to determine the stack's characteristic length. The spacing between two

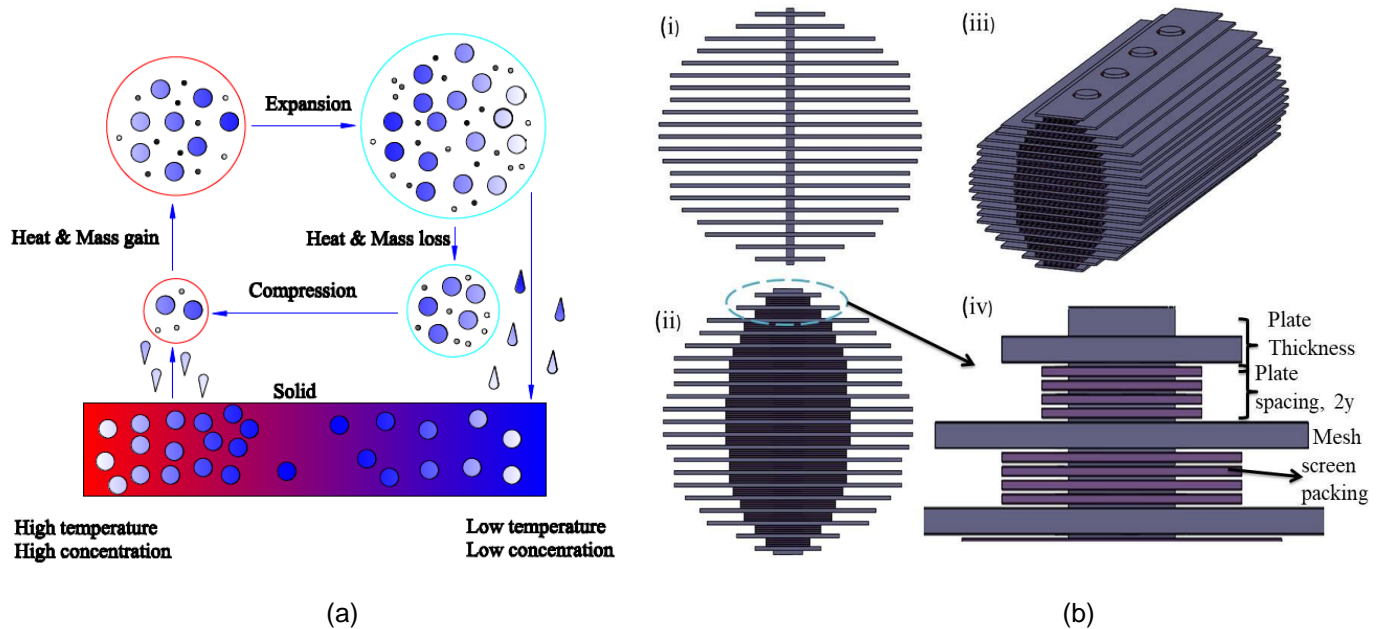


Fig. 1: (a) Conceptualized diagram depicting the working of a WTE cycle with phase change where the large and small circles are condensable component and gas, respectively. (b) Schematic of the stack showing (i) the front view of parallel plate stack (ii) the front view of modified parallel stack. (iii) Diametric view of modified parallel stack, and (iv) exploded view of modified parallel stack.

plates is defined as  $2y$ , as shown in fig.1 (b). In the parallel stack geometry,  $r_h=y$ . In WTE, the thermal penetration depth is defined as

$$\delta_k = \sqrt{\frac{2\alpha}{\omega}} \quad (1)$$

where,  $\alpha$  is the thermal diffusivity of gas and  $\omega$  is the angular frequency. Thermal penetration depth denotes the heat transfer between working fluids and a solid medium, acoustically oscillating at an angular frequency of  $\omega$ . Thermoacoustic performance is highly dependent on the ratio of hydraulic radius to thermal penetration depth,  $r_h/\delta_k$  [8]. In the modified parallel stack, as illustrated in Fig. 1(b), packing of mesh screen is added in the space between the plates and is acting both as spacer between the plates and as the retaining component of condensable liquid. Therefore, for the stack design used in this study, the spacing of parallel plates depends on the layer of the mesh screen added to the packing. Moreover, addition of heat transfer area, viscous and mass relaxation losses in the modified stack depend on mesh number and mesh packing density. These properties affect the performance of WTE significantly. Therefore, optimization of modified parallel plate was investigated by varying the plate spacing, mesh packing density, and mesh number. Fig. 2(a) and (b) show the variation of plate spacing and Fig. 2(c) and (d) demonstrate the variation of mesh packing density.

#### 4. Experimental Methods

The experimental apparatus consisted of a closed-open resonator filled with ambient air, making a quarter wavelength standing-wave thermoacoustic engine, as shown in Fig. 3(a). The resonator was made from stainless steel tube having an inner diameter of 35 mm and length of 62 cm. The system was roughly optimized to suit a 7 cm long stack which is approximately 1/10 of the total length. The stack was made from stainless steel plates. The stack was positioned at 150 mm from the closed end of the resonator, which is approximately 1/16 of the wavelength [8] at a resonant frequency of about 140 Hz at 1 atm. For these conditions, the thermal penetration depth is  $\delta_k \sim 0.22$  mm. No heat exchanger was put inside the resonator to avoid viscous dissipations. Heating was achieved by constant flow butane torch which provided a constant heat rate of 108 W, measured by flame calorimetry. The cold heat exchanger was fabricated by winding copper pipes around the duct at the cold end of the stack covering a total length of 2.5 cm. Circulating water at ambient temperature

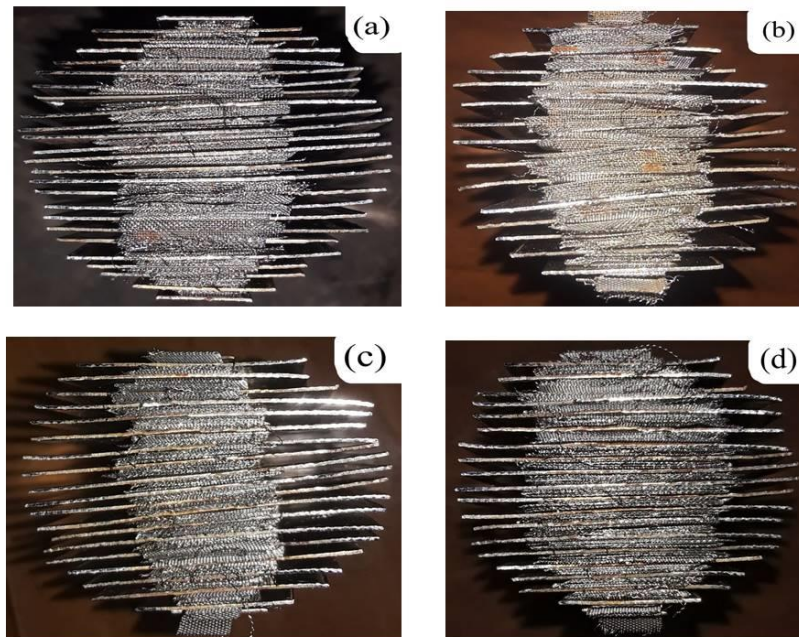


Fig. 2: Photographs of the modified parallel stack having (a)  $r_h/\delta_k=2.02$  and (b)  $r_h/\delta_k=3.27$  at a constant mesh packing density of 50%. The bottom figures show the modified parallel stack of mesh packing density (c) 30% and (d) 70% at a constant  $r_h/\delta_k$  of 2.63.

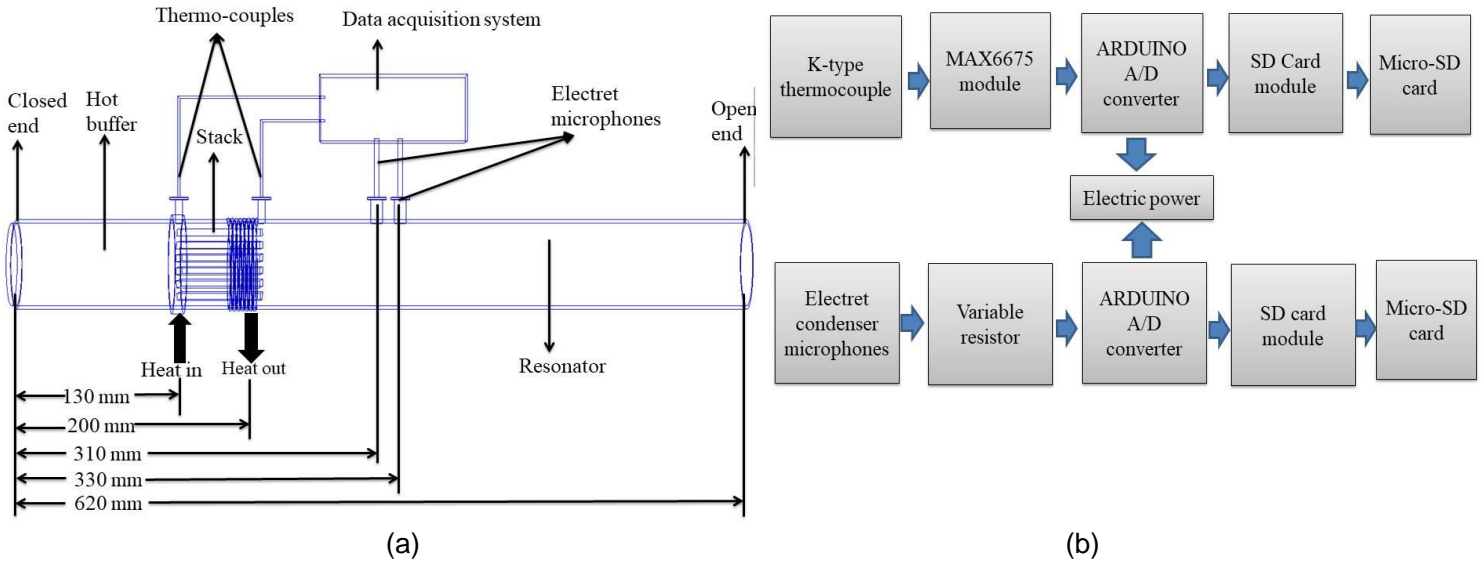


Fig. 3: (a) Schematic of the experimental setup, and (b) ARDUINO-based data acquisition system for the measured pressure and temperature.

was the cooling liquid. Temperature was measured via K-type thermocouples which were located at the two end of the stack and had an accuracy of  $1 \pm 0.5^\circ\text{C}$ . Acoustic power flux was obtained using the two-microphone method [13]. For this, two electret condenser microphones were inserted at the middle of the resonator with a distance of 20 mm between them. These microphones were calibrated using digital sound level calibrator and could measure pressure amplitude up to 80 Pa with an error band of  $\pm 2$  Pa at the maximum pressure, which was well within the range of our pressure amplitude measurements. Temperature and pressure data were stored in SD cards via ARDUINO based data acquisition system shown in Fig. 3(b). To measure the acoustic power, the acoustic power flux was multiplied by the cross-sectional area of the resonator.

The experimental procedure began by inserting the stack in the resonator. Then resonator was flooded with distilled water for soaking the stack for 5 min and then the channels of the stack and the resonator were cleared of excess water by keeping the resonator upside-down for another 10 min. This way only mesh screen packing within the stack wall remained soaked and the stacks were consistently found to retain similar mass of water (2~3 gm). After that, heating was initialized and was maintained at a constant rate. A range of experiments was performed by changing the mesh packing density, mesh number, and plate spacing of the modified parallel stack systematically. Each experiment was repeated three times and the average value of them was taken (excluding the outliers). Since there is variability of acoustic power with temperature, average values were taken into consideration to compare the performance with different stacks. Heating was turned off when the acoustic wave stopped spontaneously due to the partial drying of the stack.

## 5. Results and Discussion

### 5.1. Transient operation of the WTE

A representative experiment is presented in Fig. 4 showing the time evolution of temperature and acoustic power in a complete run of the engine. It can be seen from Fig. 4 that the acoustic power rises abruptly at a certain temperature difference along stack after the heating was initiated, indicating the onset of engine. The temperature at the hot end rises quickly, whereas the temperature at the cold end increases a little. Sharp rise of cold end temperature can be seen, as demonstrated in Fig. 4, close to the shut-down of oscillation. Oscillation induces forced convective heat transfer which absorbs heat from the cold end of stack. When oscillation stops, the cooling effect decreases, resulting in a sudden rise of

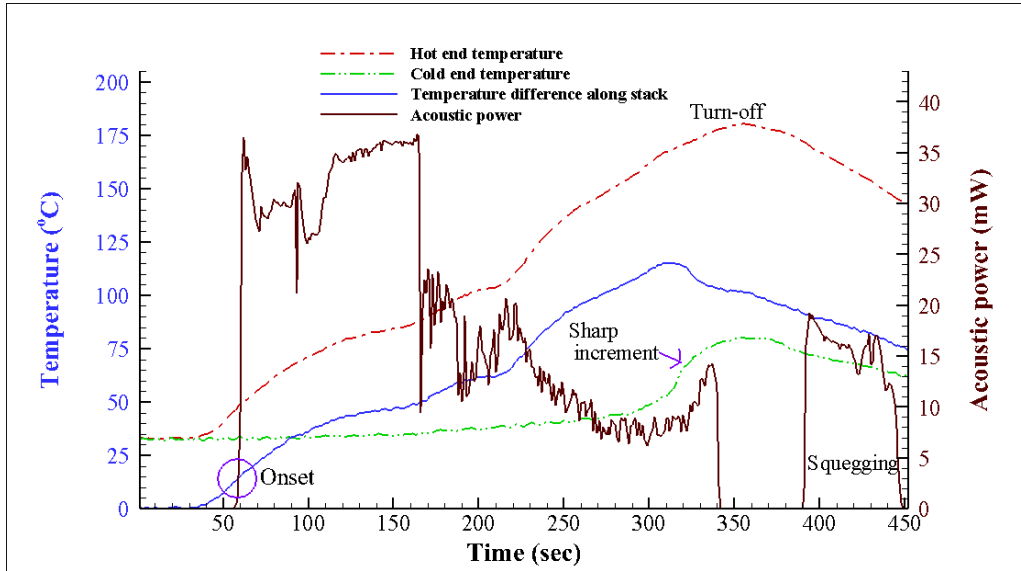
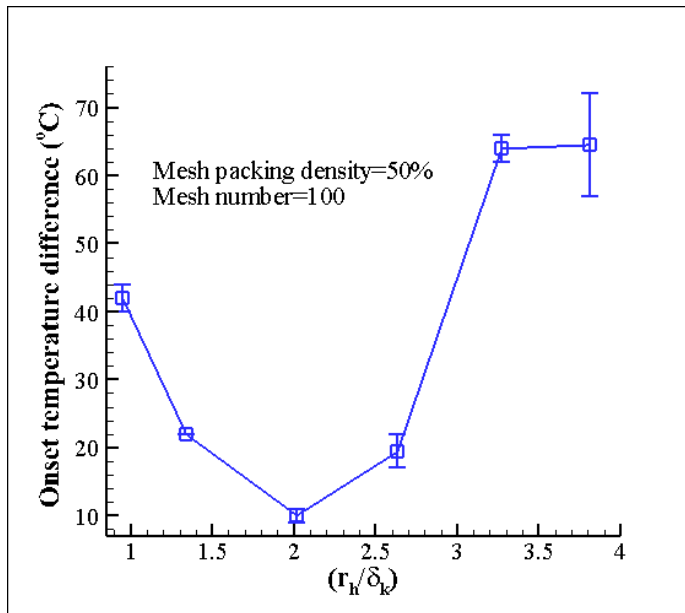
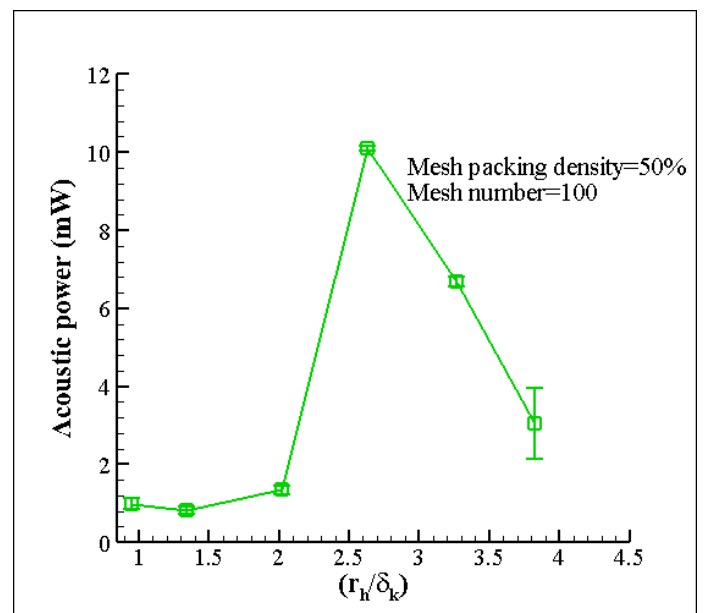


Fig. 4: Time history of temperatures (Hot end temperature, cold end temperature and temperature difference between the hot and cold end), and acoustic power during a complete run of a representative experiment.

the cold end temperature. When the heating is turned off, oscillation starts again and diminishes quickly, called the squegging effect. This can be attributed to the initiation of acoustic cycle due to the remaining vapor inside the stack with a decrease of the cold end temperature which then diminishes quickly because of a reduction of the hot end temperature.



(a)



(b)

Fig. 5: Effect of plate spacing, represented by the ratio of hydraulic radius to thermal penetration depth, on the (a) onset temperature difference, and (b) acoustic power at a constant mesh packing density=50% and mesh number=100.

### 5.2. Effect of plate spacing on the performance of WTE

The effect of plate spacing is determined by using the ratio of hydraulic radius to the thermal penetration depth. Fig. 5(a) depicts the influence of this ratio on the onset temperature difference. The onset temperature difference shows a parabolic pattern with low onset temperature difference in the range 10-22°C at 1.34-2.63  $\delta_k$ . Fig. 5(b) shows the relation between acoustic power and  $r_h/\delta_k$ . The optimum acoustic power of 10 mW was measured at 2.63 $\delta_k$ . Both the viscous dissipation and the heat transfer area decrease with an increment of plate spacing. Viscous dissipation causes acoustic power loss whereas heat transfer area increases interaction of heat with working fluids, resulting in an increment of acoustic power generation. Therefore, there is an optimum ratio of plate spacing which mediates between the viscous loss and the heat transfer area. This optimum plate spacing for this study was found at  $r_h/\delta_k=2.63$  where the maximum acoustic power was obtained at a relatively low temperature difference. This value of hydraulic radius was within the well-established range of 2~4 $\delta_k$  for dry thermoacoustic engines [10].

### 5.3. Effect of mesh packing density on the performance of WTE

The onset temperature difference as a function of mesh packing density for a constant mesh number and plate spacing is shown in Fig. 6(a). These results demonstrate that when mesh packing density increases from 20% to 40%, the onset temperature difference decreases considerably from 144 to 8°C. The onset difference remains fairly constant, with a minor variation due to the atmospheric effect, in the range of 6-24°C when mesh packing density is further increased to 50-90%. This is because increasing the packing density introduces more condensable vapour while reducing heat loss, thus resulting in a reduction of the onset temperature difference required for inducing self-oscillation. The relatively constant low onset temperature difference at 50-90% mesh packing density can be ascribed to the fact that the onset temperature difference does not change after a certain humidity ratio, as also reported by Tsuda and Ueda [6]. Due to the dominating viscous and mass relaxation dissipation at 100% mesh packing density, which make the thermo-acoustic engine difficult to oscillate, the onset temperature difference in this case increases

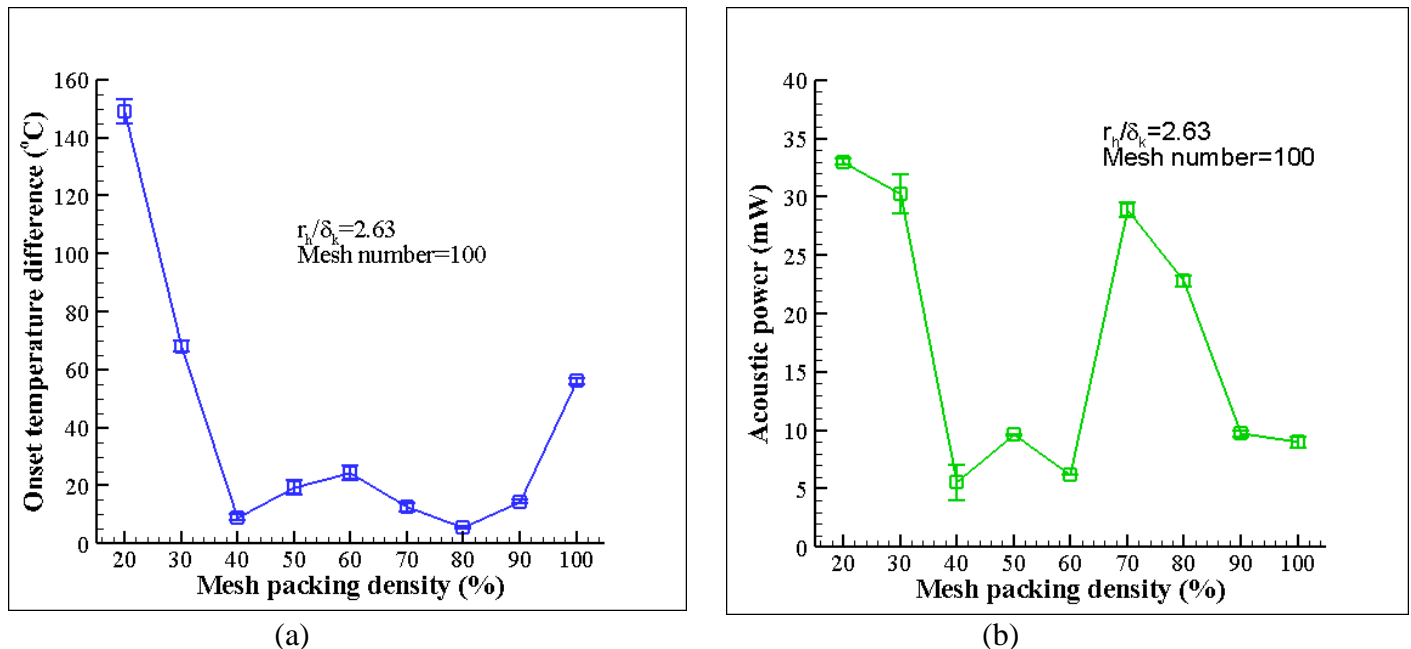


Fig. 6: Influence of mesh packing density on the (a) onset temperature difference, and (b) acoustic power at constant  $r_h/\delta_k=2.63$  and mesh number=100.

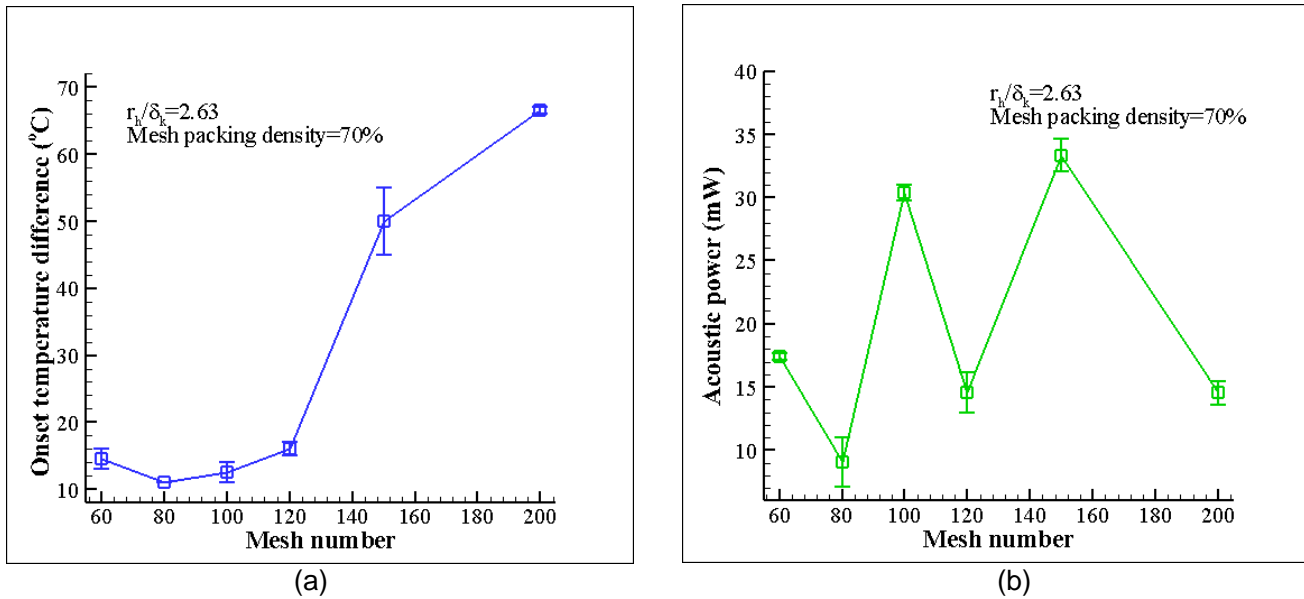


Fig. 7: The variation of (a) onset temperature difference, and (b) acoustic power as a function of mesh number at constant  $r_h/d_k=2.63$  and mesh packing density=70%.

again to 56°C. Fig. 6(b) illustrates the effect of mesh packing density on the acoustic power generated by the engine. From 20% to 30% mesh packing density, acoustic power is relatively high. This is due to the stacks' greater conversion capability at higher temperature differences. As low onset temperature difference possesses low conversion efficiency, acoustic power is low for a packing density in the range of 40-60%. Enhancement of imbibing water and heat transfer area with the increment of mesh packing density improves the performance and shows generation of acoustic power of 29 and 23 mW at 70% and 80% of mesh packing density, respectively. Eventually, the generation of acoustic power is reduced with further increment of mesh packing density because of the dominance of the viscous and mass relaxation resistances.

#### 5.4. Effect of mesh number on the performance of WTE

The mesh number is a commonly used parameter for mesh screens which indicates the fineness of a mesh. A higher mesh number means a greater number of openings per linear inch of the screen. As shown in Fig. 7(a), the onset temperature difference remains as low as 11-16°C for mesh numbers 60-120 and increases considerably to 50°C and 67°C for mesh numbers 150 and 200, respectively. These can be attributed to the dominance of mass relaxation losses at higher imbibing capability of liquid in mesh packings for mesh numbers 150 and 200, as shown in Table 1. On the other hand, the acoustic power changes abruptly with mesh number because of the abrupt change of viscous resistance, heat transfer area and mass relaxation losses (Fig. 7(b)). This variation of acoustic power with mesh number is explained further below.

Table 1 shows the heat transfer area, viscous resistance, and the percentage of open area of mesh screen packing with their mesh number at packing density of 70%. The product of the percentage of open area and the number of mesh layers ( $O \times n$ ) refers to the amount of fluid that can be imbibed into the mesh packing as fluid can be absorbed in those areas by capillary action. Because of the large open area of the imbibing liquid, mesh 150 and mesh 200 suffer from significant mass relaxation losses. On the other hand, meshes having mesh number 60, 120, and 150 have a higher viscous resistance than others which depends on hydraulic radius and porosity. From Table 1, it can be seen that the mesh number 100 possesses relatively high heat transfer area with low viscous and mass relaxation resistances, thus yielding the optimal performance of 29 mW acoustic power at a relative low onset temperature difference of 13°C. Mesh 150 also shows good acoustic power generation of 32 mW because of its higher heat transfer area, but at a high onset temperature difference of 50°C.

Table 1: Relative properties of mesh screen packing for various used mesh number at mesh packing density=70% measured using formulas derived by Swift and Ward [14] and used by Prasad [15].

Mesh number	Diameter (nm)	Number of mesh layers in the packing, n	Hydraulic radius (nm)	Porosity (%)	Heat transfer area (mm <sup>2</sup> ×10 <sup>4</sup> )	Viscous resistance (Pa.s/m <sup>3</sup> ×1 <sup>10</sup> )	Percentage of open area O (%)	O×n
60	250	3	29.1	31.80	3021	1.652	16.76	50.30
80	179	3	51.8	53.66	2867	0.076	19.02	57.09
100	149	4	31.5	45.80	4028	0.440	17.09	68.36
120	125	6	14.1	31.07	6107	7.490	16.76	100.59
150	99	7	14.5	36.98	7049	4.385	17.25	120.76
200	74	7	20.9	52.99	7035	0.505	17.42	121.91

## 6. Conclusion

A novel modified parallel plate stack is proposed, and its performance is investigated experimentally for a quarter standing wave WTE. The modified stack design consisted of parallel plates, widely used for dry thermoacoustic engines, with mesh screens for imbibing the liquid which is essential for the operation of WTE. With a view to determine the optimum design parameters, the onset temperature difference and acoustic power of the WTE were determined for various configurations of the modified stack by changing the stack parameters such as plate spacing, mesh packing density, and mesh number. Within the parametric space of this study, the optimized performance of the WTE is achieved by adopting a plate spacing of  $2.63\delta_k$ , mesh packing density of 70% and a 100-mesh at an onset temperature difference of 13°C and acoustic power of 29 mW. The obtained results with the proposed novel stack design show considerable potential for the efficient operation of WTE.

## References

- [1] G.W. Swift, *A unifying perspective for some engines and refrigerators*, Melville: Acoustical Society of America, 2002.
- [2] M. Hatazawa, H. Sugita, T. Ogawa and Y. Seo, "Performance of a thermoacoustic sound wave generator driven with waste heat of automobile gasoline engine," *Trans. Jpn. Soc. Mech. Eng.*, vol. 70:pp. 292-299, 2004.
- [3] C. Shen, Y. He, Y. Li, H. Ke, D. Zhang and Y. Liu, "Performance of solar powered thermoacoustic engine at different tilted angles," *Appl. Therm. Eng.*, vol. 29, pp. 2745-2756, 2009.
- [4] R. Raspet, W.V. Slaton, C.J. Hickey, and R.A. Hiller, "Theory of inert gas-condensing vapor thermoacoustics: propagation equation," *J. Acoust. Soc. Am.*, vol. 112, pp. 1414-1422, 2002.
- [5] D. Noda, and Y. Ueda, "A thermoacoustic oscillator powered by vaporized water and ethanol," *Am. J. Phys.*, vol. 81, no. 2, pp. 124-126, 2013.
- [6] K. Tsuda, and Y. Ueda, "Abrupt reduction of the critical temperature difference of a thermoacoustic engine by adding water," *AIP Adv.*, vol. 5, no. 9, pp. 097173, 2015.
- [7] A. Meir, A. Offner, and G. Z. Ramon, "Low-temperature energy conversion using a phasechange acoustic heat engine," *Appl. Energy*, vol. 231, pp. 372-379, 2018.
- [8] Z. Yu, A. J. Jaworski, and A. S. Abduljalil, "Impact of Viscous and Heat Relaxation Loss on the Critical Temperature Gradients of Thermoacoustic Stacks," *World. Acad. Sci. Eng. Technol.*, vol. 37, pp. 88-94, 2009.
- [9] N. M. Hariharan, P. Sivashanmugam, and S. Kasthurirengan, "Influence of stack geometry and resonator length on the performance of thermoacoustic engine," *Appl. Acoust.*, vol. 73, pp. 1052-1058, 2012.
- [10] H. Ke, Y. He, Y. Liu, and F. Cui, "Mixture working gases in thermoacoustic engines for different applications," *Int. J. Thermophys.*, vol. 33, pp. 1143-1163, 2012.
- [11] Wang, Yaxiong, and G. P. Peterson, "Investigation of a novel flat heat pipe," *J. Heat Transfer*, vol. 127, no. 2, pp. 165-170, 2005.
- [12] M. Senga., and S. Hasegawa, "Energy conversion of thermoacoustic engines with evaporation and condensation," *Int. J. Heat Mass Transf.*, vol. 165, pp. 120385, 2021.

- [13] Biwa, Tetsushi, Y. Tashiro, H. Nomura, Y. Ueda, and T. Yazaki, "Experimental verification of a two-sensor acoustic intensity measurement in lossy ducts," *J. Acous. Soc.*, vol. 124, no. 3, pp. 1584-1590, 2008.
- [14] Swift, G. W., and W. C. Ward, "Simple harmonic analysis of regenerators," *J. Thermophys. Heat Tr.*, vol. 10, no. 4, pp. 652-662, 1996.
- [15] Prasad, S. Bhushan, J. S. Saini, and K. M. Singh, "Investigation of heat transfer and friction characteristics of packed bed solar air heater using wire mesh as packing material," *Sol. Energy*, vol. 83, no. 5, pp. 773-783, 2009.